A Li-Ion Battery Charger With Smooth Control Circuit and Built-In Resistance Compensator for Achieving Stable and Fast Charging

Article *in* Circuits and Systems I: Regular Papers, IEEE Transactions on · February 2010

DOI: 10.1109/TCSI.2009.2023830 · Source: DBLP

3 authors, including:

Ke-Horng Chen
National Chiao Tung University
341 PUBLICATIONS **4,055** CITATIONS

SEE PROFILE

A Li-Ion Battery Charger With Smooth Control Circuit and Built-In Resistance Compensator for Achieving Stable and Fast Charging

Chia-Hsiang Lin, Chun-Yu Hsieh, and Ke-Horng Chen, *Senior Member, IEEE*

***Abstract*—A built-in resistance compensator (BRC) technique is presented to speed up the charging time of a lithium-ion battery. A smooth control circuit (SCC) is proposed to ensure the stable transition from the constant-current (CC) to the constant-voltage (CV) stage. Due to the external parasitic resistance of the Li-ion battery-pack system, the charger circuit switches from the CC to the CV stage without fully charging the cell. The BRC technique dynamically estimates the external resistance to extend the CC stage. The experimental results show that the period of the CC stage can be extended to 40% of that of the original design. The charging time is effectively reduced.**

***Index Terms*—Built-in resistance compensator (BRC), charger, fast charging, Li-ion cell, smooth control circuit (SCC).**

I. Introduction

NOWADAYS, portable devices have become the main applications of advanced technical products. Due to their small size, lightweight, and rechargeability, Li-ion batteries are well suited to portable electronic manufactures such as cell phones and PDAs [1]. Moreover, Li-ion batteries can store much more energy than Ni–Cd batteries with the same weight and volume. However, the life cycles of Li-ion batteries are easily affected by undercharging or overcharging [2], [3]. The reason is that overcharging may damage the physical component of the battery. On the other hand, undercharging may reduce the energy capacity of the battery. Thus, to prevent the battery from overcharging, the charging process needs to switch from the constant-current (CC) to the constant-voltage (CV) stage in order to charge the battery by a degrading current [4], [5]. However, this decision to switch from the CC to the CV stage is a serious issue for the charger because the external resistance, which may vary from 150 to 300 $\mathrm{m}\Omega$ according to related documents on the Li-ion cell battery, may cause the operation mode between the two stages to switch backward and forward. If the transition time is too early, the charging current drastically decreases, and thus, the charging time of the Li-ion battery is prolonged. Contrarily, if the transition time is too late, the large charging current may cause the battery voltage to become too high, thus damaging the battery. In other words, the suitable transition time of the two stages affects not only the charging time but also the life-cycle times of the battery.

In the conventional design of a charger, the transition time of two stages is decided by the result of the comparator when the voltage at the output of the charger is higher than a predefined value. The comparator switches the operation stage from the CC to the CV stage when the voltage at the output of the charger is raised to the default value. However, this specified voltage level of the Li-ion battery pack varies with the charging current due to the voltage drop across the external resistance. It is very difficult to define the transition voltage level because the voltage drop varies with the values of the charging current and external resistance, which, in turn, varies with the structure of the Li-ion battery pack. Furthermore, the external resistance is also temperature dependent. That is, the value of external resistance increases when the temperature of the Li-ion battery pack increases. This is a hindrance to accurately predict the correct transition voltage[6], [7]. It implies that the usage of a comparator to determine the entrance point of the CV stage is not adequate.

As shown in Fig. 1, the battery-pack system includes a Li-ion cell, protection circuits, and the external resistance [8]. The protection IC includes the circuits for overcharged protection, overheated monitor, and so on. In the charging process, the existence of external resistance prolongs the charging time. Obviously, the external resistance includes contacts, fuses, PCB trace wires, and cell resistance. Fig. 2 shows the conceptual schematic of the whole Li-ion battery-charging system. How to reduce the effect of external resistance is the main concern of the proposed method. Therefore, the components of the battery pack are represented by series resistance, while others are neglected. The charger IC is simply reshown inFig. 2. Resistors R_1 and R_2 are used to feed back the battery voltage. The final voltage level of the battery is regulated by operation amplifier VA. The voltage at the battery cell (V_{BATO}) is smaller than that at the output of the charger. Certainly, it is very difficult to predict when the Li-ion battery cell is fully charged precisely owing to the external resistance. Therefore, a smooth control circuit (SCC) and a built-in resistance compensator (BRC) are proposed in this paper for the stable and fast charging of the Li-ion battery.

The fundamental charging process is described inSection II. Furthermore, the SCC is presented to ensure the smooth transition between two different charging stages. Section III intro-

Manuscript received January 12, 2009; revised March 09, 2009. First published June 02, 2009; current version published February 10, 2010. This work was supported by the National Science Council, Taiwan, under Grant NSC 96-2221-E-009-240. This paper was recommended by Associate Editor F. Lustenberger.

The authors are with the Department of Electrical and Control Engineering, National Chiao Tung University, Hsinchu 300, Taiwan (e-mail: khchen@cn.nctu.edu.tw).

Color versions of one or more of the figures in this paper are available online at http://ieeexplore.ieee.org.

Digital Object Identifier 10.1109/TCSI.2009.2023830

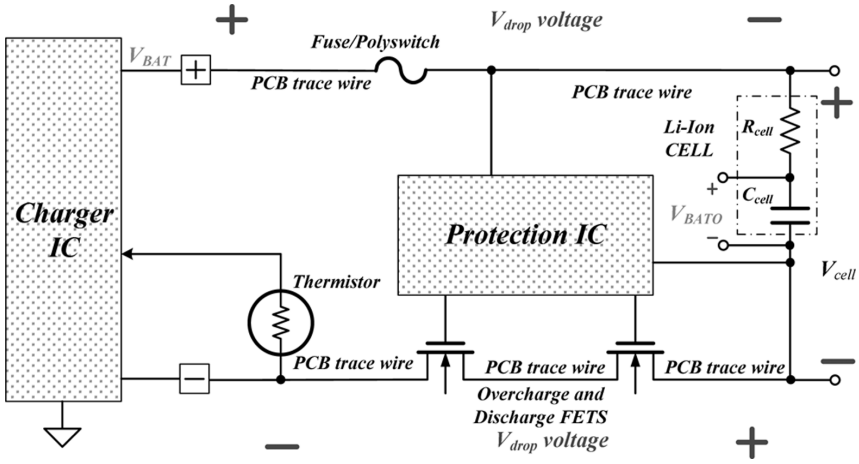

Fig. 1. Whole package of the charger IC and battery.

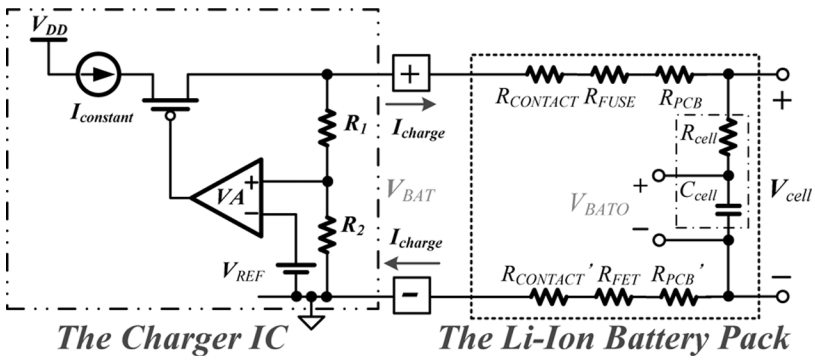

Fig. 2. Simplified circuits of the charger IC and battery.

duces the new BRC technique to achieve a fast-charging scheme in the charger design. The experimental results demonstrating the performance in terms of fast charging and smooth transition are shown in Section IV. Finally, the conclusions are illustrated in Section V.

II. Fundamental Charging Process

Generally speaking, the charging process of a Li-ion battery charger is divided into three charging stages, namely, trickle-current (TC), CC, and CV stages, as listed in Table I. The rate of charge or discharge is expressed in relation to the capacity of the battery. This rate is the so-called C-rate and equates to a charge or discharge current. When a battery is discharged at a C-rate of one, the battery consumes the nominal-rated capacity by discharging a current of 1 A in 1 h. If voltage $V_{\rm BAT}$ is smaller than the specified voltage $V_{\rm REF}$ (normally 2.5 V), the charger starts from the TC stage with a trickle charging current to avoid damage due to the large charging current on the battery. Once the value of $V_{\rm BAT}$ is larger than that of $V_{\rm REF}$, the charging process is switched from the TC to the CC stage. The charger operates at the CC stage with a constant and large driving current until the value of $V_{\rm BAT}$ exceeds that of $V_{\rm FULL}$ (normally 4.2 V), which is a predefined transition voltage, thereby entering the CV stage. The charger then charges the cell in degrading current to the full capacity until the process stops. There are two methods to terminate the charging process. One is monitoring the minimum charging current at the CV stage. The charger completes the charging process when the charging current is decreased to the specified range. To finish the charging process, the other one is based on the maximum charging time[9]. In the proposed design, the charger adopts the first method to terminate the charging process when the charge current is diminished to 0.05 C.

TABLE I
Three Operating Modes of a Conventional Charger

V_{BAT}	*Charging Process*	*Charging State*
$< V_{REF}$	**Trickle Current (TC)**	**Low charging current**
$> V_{REF}$, $< V_{FULL}$	**Constant Current (CC)**	**Larger, well-regulated current**
$> V_{FULL}$	**Constant Voltage (CV)**	**Constant Voltage & Low current**

A simplified diagram of a Li-ion battery charger is shown in Fig. 3. Referring to Fig. 2, resistance $R_{\rm pack}$ is defined as

$$R_{\rm pack} = R_{\rm CONTACT} + R_{\rm FUSE} + R_{\rm PCB} + R'_{\rm CONTACT} + R_{\rm FET} + R'_{\rm PCB} + R_{\rm cell}. \quad (1)$$

When the charger operates at the TC and CC stages, the battery is charged with a constant current decided by the values of $V_{\rm SET}$ and$R_{\rm SET}$. That is, the closed loop is established by the amplifier (MA) and OTA (CA) [10]. Thus, the value of $V'_{\rm SET}$ is

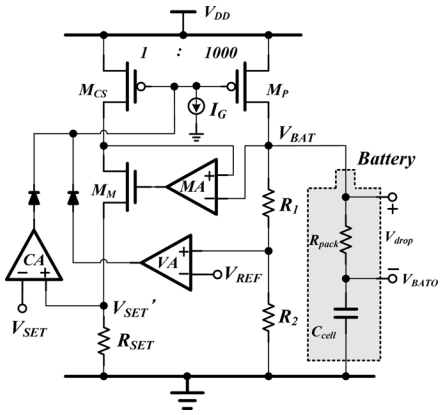

Fig. 3. Structure of a basic charger circuit [11].

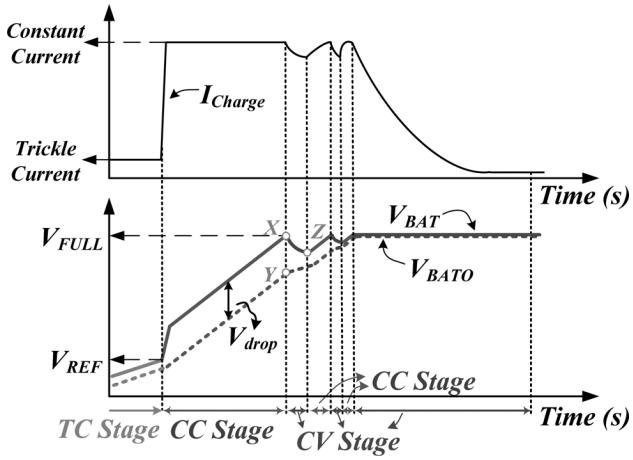

Fig. 4. Waveform of the unstable transition between the CC and CV stages due to the $V_{\rm drop}$ voltage of the battery pack.

close to that of $V_{\rm SET}$ through the virtual short of CA. Furthermore, the value of $V_{\rm SET}$ at the TC stage is set relatively smaller than that at the CC stage. The charging current at the TC stage is smaller than that at the CC stage to precharge the cell. The trickle current at the TC stage protects the battery from being damaged under a low-battery-voltage condition. When the battery is charged to an adequate voltage of 2.5 V, the charging process is switched to the CC stage automatically. Once the charging process enters the CC stage, the voltage drop across $R_{\rm pack}$ immediately increases because the charging current at the CC stage is larger than that at the TC stage. Thus, the battery voltage increases to a value above the 2.5-V transition level. The charging process enters the CC stage and never comes back to the TC stage again if the charging process continues, and the voltage of the cell drops below 2.5 V.

Similarly, the charging current at the CC stage is larger than that at the CV stage. This means that much energy is rapidly stored in the battery during the CC stage. When the battery voltage reaches the rated voltage$V_{\rm FULL}$ (4.2 V), the operating process is switched to the CV stage. However, it is too early to enter the CV stage because the battery voltage is the summation of the voltage at the battery cell $(V_{\rm BATO})$ and the$V_{\rm drop}$ voltage. At the CV stage, operation amplifier VA with M_P, R_1, and R_2 acts as a linear regulator and generates a gradually decreasing current, which may minimize the possibility that the charger will be switched between the CC and CV stages. However, the disappearance of the large $V_{\rm drop}$ voltage at the CV stage still causes the charger to have an unstable condition, as conceptually shown in Fig. 4.

The comparator, which compares the voltage at the battery pack and the predefined voltage $V_{\rm FULL}$, causes the early entrance of the CV stage. In Fig. 4, point X represents the voltage at the battery pack ($V_{\rm BAT}$), and point Y stands for the voltage at the battery cell ($V_{\rm BATO}$). The output of the comparator can decide the transition point of the charging stage but cannot account for the effect of external resistance when the predefined rated voltage $V_{\rm FULL}$ is set to 4.2 V. Furthermore, due to the gradually decreasing charging current, to avoid overcharging, the voltage at the battery pack $(V_{\rm BAT})$ will become smaller than the predefined rated voltage$V_{\rm FULL}$. At this time, the charging process comes back to the CC stage once again because the voltage at the battery pack is decreased to point Z in Fig. 4. The oscillation will continue many times until the voltage at the battery cell is close to the rated voltage $V_{\rm FULL}$. The hysteretic comparator is often used to avoid the aforementioned problem. However, the range of hysteresis is the key factor of the design. The drop in$V_{\rm BAT}$ is decided by the charging current and external resistors. If the range is too large, the charger enters the CV stage too early, and the charging time is prolonged relatively. Contrarily, if the range is too small, the hysteresis is useless to help avoid the oscillation. There are two disadvantages that exist in the aforesaid charger design. One is the longer charging time due to the early entrance of the CV stage. The other one is the unstable transition between the two stages.

In an attempt to minimize the error due to the external resistance in the Li-ion battery-pack system, commercial charger circuits use external compensation resistors to compensate for the $V_{\rm drop}$ voltage[12]. The major disadvantage is that the module of the charger is too large to be compact for portable devices. Moreover, compensation resistors cannot be adapted to the variations in external resistance in the Li-ion battery-pack system due to the thermal effect. Therefore, the BRC is proposed in this paper to make the module of the charger compact and to prolong the period of the CC stage. Owing to the longer duration at the CC stage and the shorter duration at the CV stage, the Li-ion cell can be charged to more closely approach the rated voltage even if the external resistance in the Li-ion battery-pack system varies with the thermal effect. The behavior of the proposed charger with the BRC technique in the presence of the shorter duration of the CV stage can effectively shorten the charging time of the battery.

In this paper, the decision of the charging transition is an analogy method in order to have a smooth transition between the CC and CV stages. The analogy control method is achieved by the SCC technique. Referring toFig. 5, the SCC contains current mirrorsM_1 and M_2, pass transistor $M_{\rm CA}$, and current source I_G. The current loop is controlled by the amplifier (MA) and OTA (CA), while the voltage loop is controlled by amplifier VA. At the beginning of the charging process, the voltage at the battery pack is low and causes the output of amplifier VA to be high enough to turn off transistor$M_{\rm VA}$. Thus, the voltage

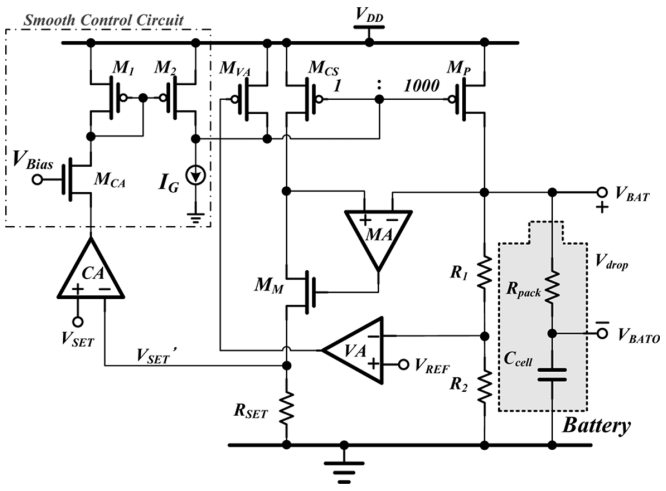

Fig. 5. Simplified diagram of the charger based on the analogy method.

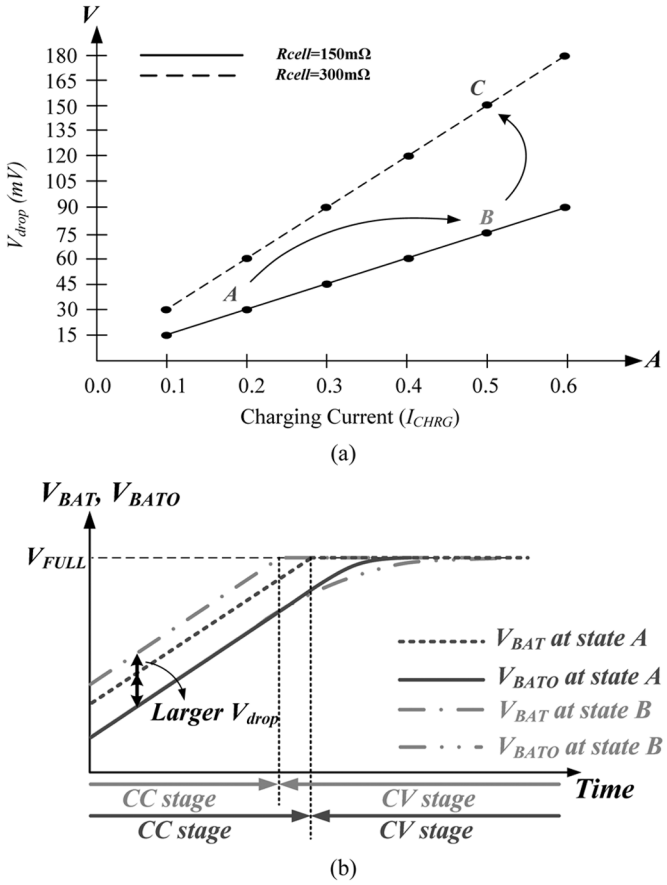

Fig. 6. $V_{\rm drop}$ voltage under a different charging current and $R_{\rm pack}$. (a) $V_{\rm drop}$ voltage is affected by the product of the charging current and external resistance. (b) Charging timing diagrams of points A and B in (a).

loop has no effect on the charging current. That is, the charging current, which is equal to $V_{\rm SET}/R_{\rm SET}$, is controlled by the current loop. Once voltage $V_{\rm BAT}$ approached the rated $V_{\rm FULL}$, the output voltage of amplifier VA becomes low enough to turn on transistor $M_{\rm VA}$ to overcome constant current I_G. Therefore, the voltage at the gate of power MOSFET M_P is also raised to a voltage level to decrease the current flowing through transistor $M_{\rm CS}$. Voltage $V'_{\rm SET}$ is decreased to cause the output of OTA (CA) to be high enough to turn off pass transistor $M_{\rm CA}$. Therefore, there is no current flow through current mirrors M_1 and M_2, and the current loop is turned off automatically. Then the charging process is smoothly switched from the CC stage to the CV stage by SCC. That is, there would be no oscillation between the CC and CV modes during the transition period. At the CV stage, operation amplifier VA takes control of the charger, and this charger acts as a linear regulator. It also keeps the battery at a regulated voltage $V_{\rm FULL}$ until the charging process is terminated.

The analogy method may solve the unstable transition problem existing in conventional design. However, the early entrance of the CV stage still exists owing to the external resistance. A large charging current causes the large $V_{\rm drop}$ voltage across the external resistance in the Li-ion battery-pack system. It makes the charger circuit detect the transition point of the CC to the CV stage more early than that with a small charging current. The $V_{\rm drop}$ voltage is added to the $V_{\rm BATO}$ voltage at the battery cell before the $V_{\rm BATO}$ voltage is fully charged to the rated-voltage level. It indicates that the $V_{\rm drop}$ voltage affects the optimum transition point from the CC to the CV stage. In other words, it takes a long time to charge the battery to the rated voltage at the CV stage when using a large charging current in the CC stage. That is, a larger charging current at the CC stage cannot reduce the charging time because of the short CC and long CV periods. Finally, the total charging is prolonged.

In Fig. 6(a), the$V_{\rm drop}$ voltage at point B is larger than that at point A due to the larger charging current. Moreover, the voltage drop at point C is larger than that at point B due to the larger external resistance. Briefly speaking, the$V_{\rm drop}$ voltage depends on the product of the charging current and external resistance. The charging timing diagrams of points A and B in Fig. 6(a) are shown in Fig. 6(b). Obviously, the charging time is prolonged when the charging current is large due to the short CC period. That is, the duration of the CC stage plays an essential role in the evaluation of charging time. Existing charger circuits suffer from the drawback of inaccuracy of the transition point from the CC to the CV stage. To shorten the charging time, the compensation of the $V_{\rm drop}$ voltage is a critical problem to be solved. The circuit for detecting the external resistance of the battery-pack system is proposed to achieve the fast-charging technique.

III. Proposed BRC Technique

As shown in Fig. 6(a), insufficient energy is stored in the battery due to the $V_{\rm drop}$ voltage during the CV stage. Particularly, in the case of charging the battery with a large current like the movement from points A to B, the $V_{\rm drop}$ voltage becomes large, and thus, the charging time is also prolonged due to the longer CV period.

Even if the external resistance can be estimated and compensated for by an external method, its value would still vary with temperature. The increasing external resistance also increases the $V_{\rm drop}$ voltage, thereby increasing the charging time. The movement from points B to C can reveal this scenario. It means that a fixed compensation method for the external resistance is

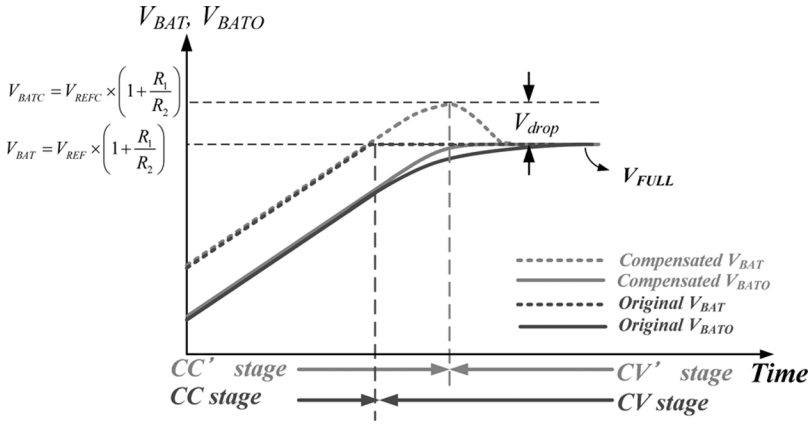

Fig. 7. Improved waveform at the end of the charging process after using the BRC technique.

still inaccurate. In other words, external-resistance compensation is needed before entering the CV stage. Certainly, the compensation method also needs to tolerate the variation in temperature.

A. Concept of the BRC Technique

The BRC technique is applied in the charging process to improve performance. As shown in Fig. 5, because the difference voltage between the $V_{\rm BATO}$ voltage at the Li-ion cell and the voltage of the battery $V_{\rm BAT}$ is the $V_{\rm drop}$ voltage, this implies that the reference voltage can be shifted to a higher voltage level, and the final voltage level of $V_{\rm BAT}$ can be redefined. The shift reference voltage is defined as $V_{\rm REFC}$, and the redefined voltage level of $V_{\rm BAT}$ is $V_{\rm BATC}$. As a result, the $V_{\rm BATO}$ voltage at the Li-ion cell can be closely approached to $V_{\rm FULL}$ at the end of the CC stage owing to the higher reference voltage. Fig. 7 shows the comparison of the charging waveform with a higher $V_{\rm REFC}$ and that with an uncompensated $V_{\rm REF}$. Obviously, the period of the original CC stage is extended to the CC$'$ stage after using the BRC technique.

To compensate for the $V_{\rm drop}$ voltage, a new reference voltage $V_{\rm REFC}$, which is the summation of incremental voltage $V_{\rm INC}$ and original reference voltage $V_{\rm REF}$, is introduced. Incremental voltage $V_{\rm INC}$ is defined as

$$V_{\rm INC} = (V_{\rm BATO} - V_{\rm BAT}) \times \frac{R_2}{R_1 + R_2} = V_{\rm drop} \times \frac{R_2}{R_1 + R_2}. \tag{2}$$

Thus, the voltage of the battery-pack system is charged to a higher voltage level at the end of the CC stage. The Li-ion battery cell can store much more energy at the CC$'$ stage for a longer period than that at the CC stage based on the original design. Once the charging process enters the CV stage, the reference voltage at the CV stage is decreased back to its original value gradually. Thus, the battery can be charged to the designated voltage $V_{\rm FULL}$ when the charging process is ended. By using the dynamic reference-voltage method, not only will the charging time be decreased, but the overcharging problem will also not occur in the charging process. Furthermore, the energy stored in the battery is not affected because the final regulated-voltage level of the battery is unchanged.

B. Estimation of External Resistance at the CC Stage

To determine the value of variable external resistance, it is important to find out a method to accurately estimate the value. As shown in Fig. 5, the $V_{\rm BATO}$ voltage at the Li-ion cell is smaller than the specified $V_{\rm FULL}$ voltage due to the $V_{\rm drop}$ voltage before the charging process is switched to the CV stage. Based on the fact that the charger charges the battery cell tardily when the battery voltage $V_{\rm BAT}$ is close to 4.2 V, the $V_{\rm BATO}$ voltage of the Li-ion cell can be viewed as a constant during a short test time.

At the beginning of the estimation, the charging current is changed from $I_{\rm CHRG1}$ to$I_{\rm CHRG2}$. It causes a voltage difference at the battery voltage $V_{\rm BAT}$ owing to the voltage drop across external resistance $R_{\rm pack}$. At the Li-ion battery pack, the two battery voltages V_1 and V_2 can be written as (3) and (4) according to the two different charging currents $I_{\rm CHRG1}$ and $I_{\rm CHRG2}$, respectively

$$V_1 = (I_{\rm CHRG1} \times R_{\rm pack}) + V_{\rm BATO1} \tag{3}$$

$$V_2 = (I_{\rm CHRG2} \times R_{\rm pack}) + V_{\rm BATO2}. \tag{4}$$

According to the previous assumption that $V_{\rm BATO1}$ and $V_{\rm BATO2}$ are equal to each other within a small charging time, external resistance $R_{\rm pack}$ can be estimated by

$$R_{\rm pack} \approx \frac{V_1 - V_2}{I_{\rm CHRG1} - I_{\rm CHRG2}}, \quad \text{assuming that } V_{\rm BATO1} \approx V_{\rm BATO2}. \tag{5}$$

Therefore, if the three parameters $I_{\rm CHRG1}$, $I_{\rm CHRG2}$, and V_1 are predefined, the value of $R_{\rm pack}$ can be determined by the estimated value of battery voltage V_2. The BRC technique provides the internal detection method to acquire the V_2 voltage.

C. Proposed Architecture of the Charger With the BRC Technique

The proposed architecture of the charger with the BRC technique is shown in Fig. 8. The compensation circuit is composed of the external-resistance detector, the reference-voltage switch circuit, and the reference shift circuit. The external-resistance detector is used to determine the value of the external resistance of the Li-ion battery pack. The $V_{\rm FB}$ feedback voltage is equal to (6). However, the $V'_{\rm BAT}$ input voltage is designed as (7) to meet

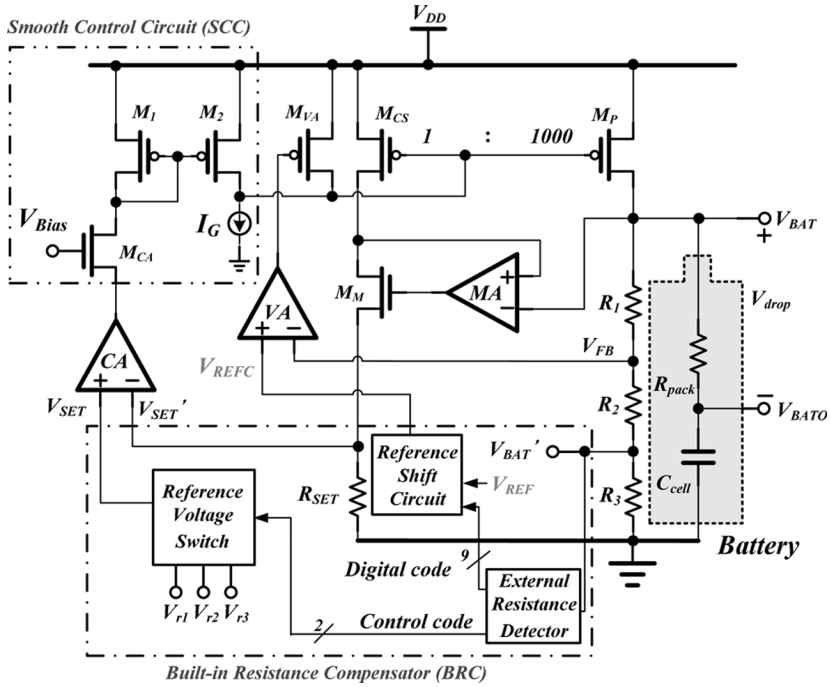

Fig. 8. Proposed fast-charging charger with external-resistance estimation.

the requirement of the headroom of the detector circuit and the supply voltage. The output of the external-resistance detector contains two parts. One part is the 9-bit digital code to determine the new reference voltage to regulate the final level of the battery. The other part is the 2-bit control code to determine the status of the estimation. The 2-bit control code decides the output voltage of the reference-voltage switch circuit during the estimation period. The estimation is designed to be at the CV stage to detect the external resistance. The variation in reference voltage in estimation does not affect the battery voltage. Finally, according to the 9-bit digital code, the reference shift circuit outputs a compensated reference voltage($V_{\rm REFC}$) to extend the period of the CC stage

$$V_{\rm FB} = V_{\rm BAT} \cdot \frac{R_2 + R_3}{R_1 + R_2 + R_3} \tag{6}$$

$$V'_{\rm BAT} = V_{\rm FB} \cdot \frac{R_3}{R_2 + R_3} = V_{\rm BAT} \cdot \frac{R_3}{R_1 + R_2 + R_3}. \tag{7}$$

For the reference-voltage switch circuit, the V_{r1} and V_{r3} input voltages are used to decide the charging current at the TC and CC stages, respectively. That is, the $V_{\rm SET}$ voltage is set to V_{r1} (or V_{r3}) at the TC (or CC) stage under a normal charging process. Undoubtedly, the value of V_{r3} is larger than that of V_{r1} to ensure a large charging current at the CC stage. Here, a new V_{r2} rated voltage is used to decide another charging current at the CC stage for external-resistance estimation. Thus, the values of the two constant charging currents $I_{\rm CHRG1}$ and $I_{\rm CHRG2}$ can defined as

$$I_{\rm CHRG1} = \frac{V_{r3}}{R_{\rm SET}} \tag{8}$$

$$I_{\rm CHRG2} = \frac{V_{r2}}{R_{\rm SET}}. \tag{9}$$

The value of voltage $V_{\rm SET}$ is maintained at the value of V_{r3} at the CC stage for conventional design. However, for the proposed charger, the value of $V_{\rm SET}$ is changed from V_{r3} to V_{r2} at a certain time (t_2) and is set back to V_{r3} at another time (t_3) at the end of the CC stage during the estimation of external resistance. The variation in the value of the $V_{\rm SET}$ voltage will cause a variation in the charging current. Consequently, the voltage at the Li-ion battery pack will also be affected due to the different $V_{\rm drop}$ voltages. That is, the $V_{\rm BAT}$ battery voltage changes from V_1 to V_2, as shown in Fig. 9. Referring to (5), the voltage of V_1 is predecided, and the voltage of V_2 needs to be estimated. To accurately detect the variable external resistance in the Li-ion battery pack, the predefined detection point is designed at $V_{\rm BAT} = V_1 = 4\,{\rm V}$. In the proposed charger, the value of $R_1 + R_2$ is equal to the value of R_3 in order to sense half the value of $V_{\rm BAT}$. According to (7), voltages V_1 and V_2 are redefined as V'_1 and V'_2, respectively. That is, the values of V'_1 and V'_2 are half the values of V_1 andV_2. Meanwhile, the value of V'_1 is equal to 2 V.

D. Proposed External-Resistance Detector and the Reference-Voltage Switch Circuit

The whole detailed circuit of the external-resistance detector is shown inFig. 10. The value of voltage $V'_{\rm BAT}$ isV'_1 at time t_2 when the Φ_1 control signal turns from low to high, and the value of voltage $V_{\rm BAT}$ reaches 4 V. Certainly, the value of voltage $V'_{\rm SET}$ is V_{r3} for defining the $I_{\rm CHRG1}$ charging current. By using a sample-and-hold (S/H) circuit, voltage V'_1 is stored on capacitor $C_{\rm SH1}$. When the value of voltage $V'_{\rm SET}$ reaches V_{r2} for defining the $I_{\rm CHRG2}$ charging current, the Φ_2 control signal turns from high to low, and the estimated value of V'_2 at time t_3 is stored in capacitor $C_{\rm SH2}$. The two values V'_1 and V'_2 are sent to the differential inputs of the G_m amplifier, which has the transconductance of $2/R_{\rm VI}$, as shown in Fig. 10(a)[13], [14].

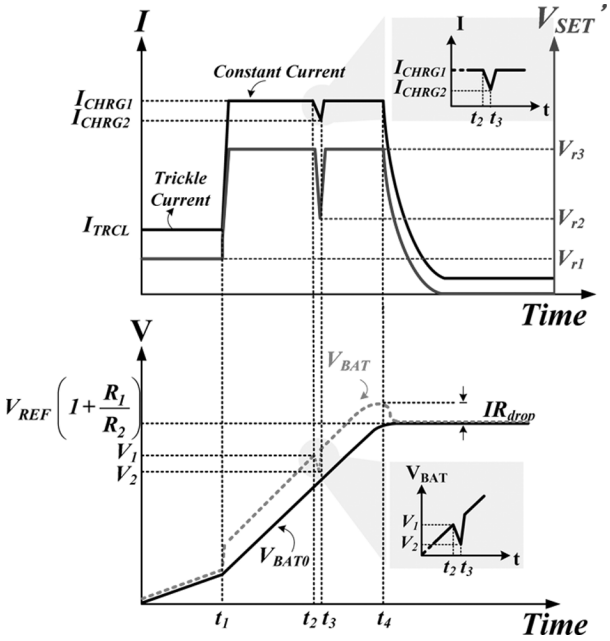

Fig. 9. Waveform of battery voltage during the detection period.

The charge injection and clock feedthrough of the S/H circuits can be ignored owing to the differential operation. Thus, the accuracy is not affected during the detection period. The value of the $I_{\rm DROP}$ output current is proportional to the difference of the two voltages V_1' and V_2'. The expression of the $I_{\rm DROP}$ current is shown in

$$\begin{aligned} I_{\rm DROP} &= G_m \cdot (V_1' - V_2') = \frac{2}{R_{\rm VI}} \cdot (V_1' - V_2') \\ &= \frac{2}{R_{\rm VI}} \cdot 2 \times (V_1 - V_2) \\ &= \frac{2}{R_{\rm VI}} \cdot 2V_{\rm drop} \propto V_{\rm drop}. \end{aligned} \tag{10}$$

As shown in Fig. 10(a), the $I_{\rm DROP}$ current is mirrored to bias the delay-line circuit inFig. 10(b)[15]. The larger external resistance causes a larger $V_{\rm drop}$ voltage, thereby resulting in a larger biasing current $I_{\rm DROP}$. Therefore, the delay time of the delay-line circuit is inversely proportional to the $V_{\rm drop}$ voltage. That is, a large $V_{\rm drop}$ voltage can be interpreted as a big digital number and vice versa. Therefore, the delay-line ADC can output a different digital code for representing the external resistance according to the various $V_{\rm drop}$ voltages. The reference shift circuit then increases reference $V_{\rm REF}$ to$V_{\rm REFC}$ according to the 9-bit digital code.

E. Proposed Reference Shift Circuit

After the estimation of the external resistance of the Li-ion battery-pack system, a 9-bit digital code generated by the external-resistance detector is sent to the reference shift circuit to add the incremental voltage $V_{\rm INC}$ to$V_{\rm REF}$ according to the value of the digital number, which is converted by the delay-line ADC in Fig. 10(b). Referring to Fig. 11, the $I_0, I_1, \ldots, I_8$, and $I_{\rm base}$ currents are determined by the value of the $V_{\rm SET}'$ voltage. The external resistance varies from 150 to 300 $\rm m\Omega$. Assuming that the minimum external resistance is 150 $\rm m\Omega$, the needed minimum compensation current is the $I_{\rm base}$ base current, which flows through resistor $R_{\rm CO}$ and decides the minimum new reference voltage$V_{\rm REFC}$. The minimum value of the $V_{\rm REFC}$ reference voltage is expressed as

$$\begin{aligned} V_{\rm REFC(min)} &= V_{\rm REF} + (I_{\rm base} \times R_{\rm CO}) \\ &= V_{\rm REF} + (150\ {\rm m\Omega}) \times I_{\rm CHRG} \times \frac{R_2 + R_3}{R_1 + R_2 + R_3} \\ &= V_{\rm REF} + \Delta V_{C1}. \end{aligned} \tag{11}$$

The value of voltage $V_{\rm ADD}$ is used to compensate for the variation in external resistance ranging from 150 to 300 $\rm m\Omega$. The value of voltage $V_{\rm ADD}$ can be expressed as (12). Finally, the $V_{\rm INC}$ incremental voltage for compensating the reference voltage is equal to the summation of voltages $V_{\rm REF(min)}$ and $V_{\rm ADD}$

$$\begin{aligned} V_{\rm ADD} &= \sum_{i=0}^{N} I_i \times R_{\rm CO} \\ &= \left[\frac{N+1}{9}\right] \times I_{\rm CHRG} \times \left(150\ {\rm m\Omega} \times \frac{R_2 + R_3}{R_1 + R_2 + R_3}\right) \\ &= (N+1) \times \Delta V_{C2}. \end{aligned} \tag{12}$$

The value of N is from zero to eight. The corresponding compensating voltages due to different digital codes are listed in Table II. Because the assumption of the smallest external impedance is 150 $\rm m\Omega$, ΔV_{C1} compensates for the fundamental $V_{\rm drop}$ of the battery-pack system that is referred to in(11). As shown in Fig. 12, the voltage of $V_{\rm REFC}$ shifts to 2.59 V when the digital code is 1111111111 because the values of currents $I_0, I_1, \ldots, I_8$, and $I_{\rm base}$ are flowing through resistor $R_{\rm CO}$. The values of currents $I_0, I_1, \ldots, I_8$, and $I_{\rm base}$ are controlled by the value of voltage $V_{\rm SET}'$. Thus, the values of these currents are gradually decreased to zero when voltage $V_{\rm SET}'$ is decreased to zero due to the decreasing current of transistor $M_{\rm CS}$ at the CV stage. As a result, the $V_{\rm INC}$ incremental voltage will be smoothly decreased to zero. The reference voltage returns to the original value at the CV stage without affecting the rated fully charged voltage.

After the implementation of the proposed charger with the BRC technique, the period of the CC stage can be extended to charge much more energy to the Li-ion battery cell faster, and the overcharge problem can also be avoided.

IV. Experimental Results

The proposed charger with the BRC technique was implemented in TSMC 0.35-μm CMOS technology. The threshold voltages of nMOSFET and pMOSFET are 0.55 and 0.65 V, respectively. Table III lists the specifications of the proposed charger.

The chip micrograph is shown in Fig. 13. The silicon area is $1300 \times 850\ \mu{\rm m}^2$. The setup of the test chip is shown in Fig. 14. The pin of EN_BRC can be set to low to turn off the BRC technique system. The supply voltage of the charger is 5 V, and the fully charged voltage $V_{\rm FULL}$ is 4.2 V. The specifications of the proposed charger are referred to the product of the charger in the

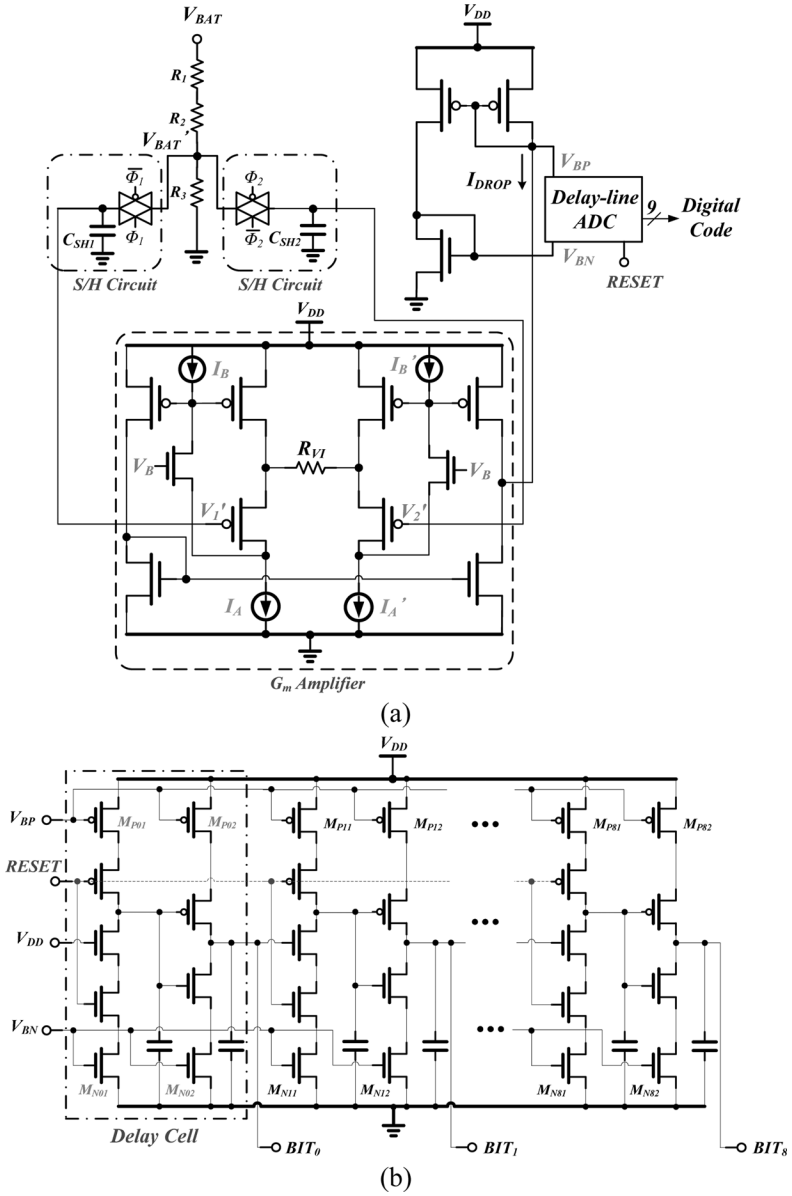

Fig. 10. (a) Schematic of the circuit of the external-resistance detector with an on-chip S/H circuit. (b) Schematic of the delay-line circuit.

market. To emulate the external resistance of the battery-pack system, one resistor $R_{\rm pack}$ of 300 $\rm m\Omega$ is used to represent the external resistance. Furthermore, to monitor the charging process within a short period, one large capacitor $C_{\rm CELL}$ of 10000 μF is used to emulate the large capacity of the Li-ion battery.

As shown in Fig. 15, the waveform of the battery cell$V_{\rm BATO}$ is presented based on an SCC. The enable signal is used to control the charging process. By adopting the current control method in the design of CA, the charger smoothly switches from the CC to the CV stage without any oscillation between the CC and CV stages. The current loop, which is composed of OTA (CA) and MA amplifiers, is gradually turned off. The charger becomes a linear regulator after the voltage loop, which is constituted by the VA amplifier, controls the charger. That is, the voltage of the Li-ion cell is charged to the rated voltage steadily.

Because the output capacitor is 10000 μF, it is easy to determine that the charging time of the TC stage is 500 ms. InFig. 16, the estimated result is similar to that obtained from the calculation. Furthermore, the periods of the CC and CC$'$ stages are 22 and 32 ms, respectively. The period of the CC stage is extended to about 40% of that of the original charger without the BRC technique. Due to the external resistance at 300 $\rm m\Omega$, the digital number of the detector is 111111111. Then, the reference shift circuit adds the max shift voltage to the $V_{\rm REF}$ reference voltage for compensating for the $V_{\rm drop}$ voltage. Thus, the $V_{\rm BATO}$ voltage at the Li-ion cell can reach the specific voltage (4.2 V) more quickly than that of the original design without the BRC technique. From the zoom-in window inFig. 16, the $V_{\rm BATO}$ voltage can be rapidly raised to 4.2 V due to the extension of the CC stage.

In Fig. 17, the $V_{\rm drop}$ voltage exists between voltages $V_{\rm BATO}$ and $V_{\rm BAT}$. The period of the CC stage can be extended from the

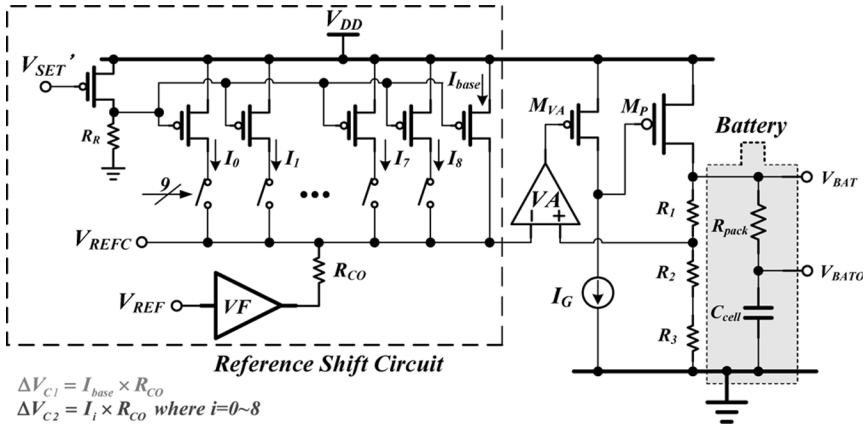

Fig. 11. Reference shift circuit generates the V_{REFC} BRC reference voltage by adding the V_{INC} incremental voltage to the V_{REF} original reference voltage.

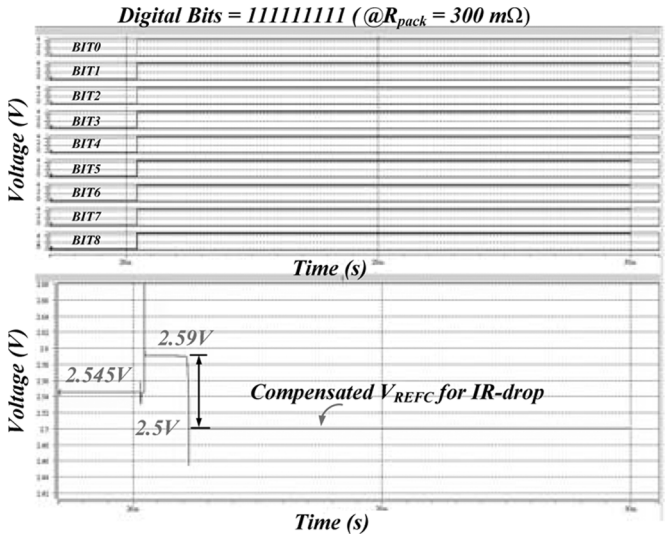

Fig. 12. Waveform of the digital bits and compensated V_{REFC} for the V_{drop} voltage.

TABLE II
CORRESPONDING VALUES OF THE V_{INC} VOLTAGE FOR DIFFERENT DISTINCT EXTERNAL RESISTANCES R_{pack}'S DERIVED FROM DIFFERENT DIGITAL CODES (THE V_{REF} REFERENCE VOLTAGE IS 2.5 V).

R_{pack} (mΩ)	Digital Code		V_{INC} (mV)	V_{REFC} (V)
150.00	000000000	1	45	2.545
166.67	000000001	1	50	2.550
183.00	000000011	1	55	2.555
200.00	000000111	1	60	2.560
216.67	000001111	1	65	2.565
233.00	000011111	1	70	2.570
250.00	000111111	1	75	2.575
266.67	001111111	1	80	2.580
283.00	011111111	1	85	2.585
300.00	111111111	1	90	2.590

CC stage to the CC″ stage because the value of the compensated V_{BAT} is larger than that of the original V_{BAT}. Because the voltage variation at the V_{BAT} voltage is very small, the V_{SET} node voltage in Fig. 8 is connected to an output to monitor the detection period. The estimated waveform of voltage V_{SET}

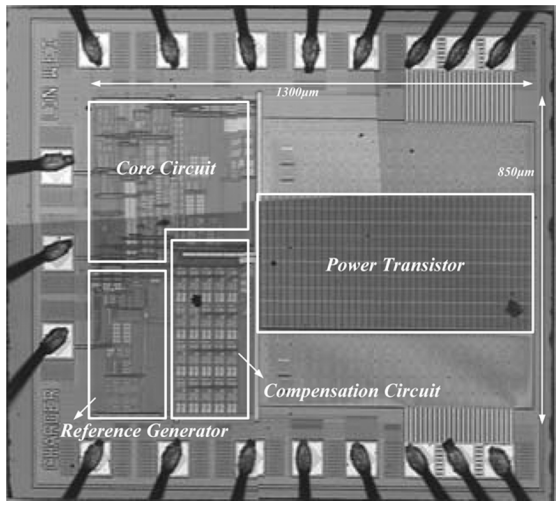

Fig. 13. Chip micrograph.

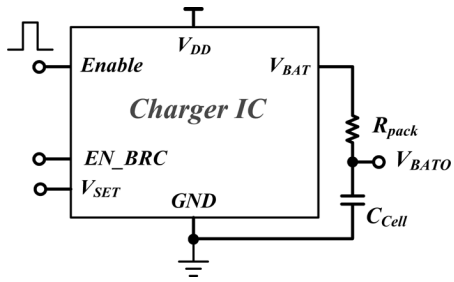

Fig. 14. Estimation setup of the proposed charger.

is shown in Fig. 18. During the detection period, the value of voltage V_{SET} is pulled low to 0.9 V for a short time and back to 1.5 V. The detection period is 0.5 ms in Fig. 18. During the detection period, the charger acquires sufficient information on the external resistance of the battery-pack system to compensate for the V_{drop} voltage.

Fig. 19 shows the estimation results of the V_{REFC} shift reference voltage. It demonstrates the linearity of the compensation voltage. Thus, the V_{REFC} shift reference voltage can be adjusted according to the the digital code. That is, the entrance time from

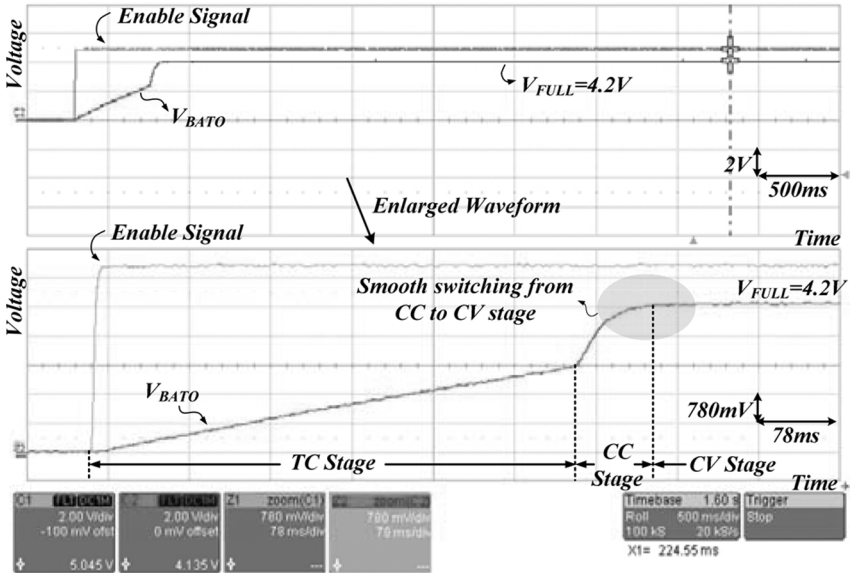

Fig. 15. Smooth charging waveform from the CC to the CV stage achieved by the analogy method.

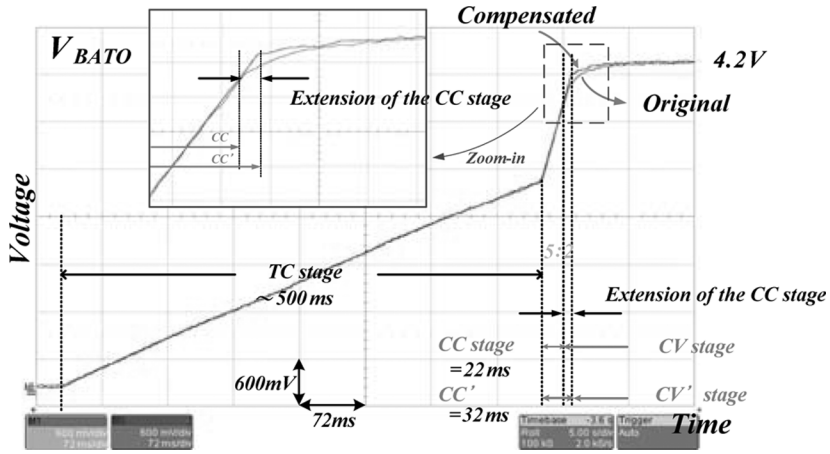

Fig. 16. Waveforms of the V_{BATO} voltage with and without the BRC technique. The CC stage of the original design is extended to the CC' stage of the BRC design.

TABLE III
SPECIFICATIONS OF THE PROPOSED CHARGER WITH THE BRC TECHNIQUE

V_{DD}	4.5 V~6.5 V
C_{cell}	10000 μF
R_{pack}	150 mΩ ~ 300 mΩ
V_{r1}	0.15 V
V_{r2}	0.9 V
V_{r3}	1.5 V
R_{SET}	3.0 KΩ
V_{REF}	2.5 V
V_{FULL}	4.2 V
V_1	4.0 V
V_1'	2.0 V
I_{CHRG0} (TC Mode)	50mA
I_{CHRG1} (CC Mode)	500mA
I_{CHRG2} (Detection Mode)	300mA

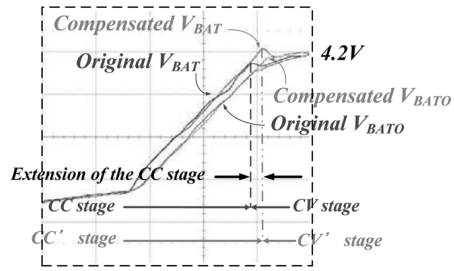

Fig. 17. Waveforms of voltages V_{BAT} and V_{BATO} with and without the BRC technique. The voltages of the compensated V_{BAT} and V_{BATO} are obtained from the BRC technique.

the CC to the CV stage can be delayed based on the external resistance of the Li-ion battery pack.

The proposed BRC method is tested by a real Li-ion battery. The battery pack used in the experimental validation has a V_{FULL} of 4.2 V, an external resistance of 150–300 $\mathrm{m}\Omega$, and a capacity of 4.2 V$\times$ 900 mA $\cdot$ h. Fig. 20 shows the experimental results of the charger with and without the BRC technique. It shows the variation in the I_{CHRG} charging current and the V_{BAT} battery voltage. The charging times of the originally designed and proposed chargers are about 2.5 and 2.0 h, respectively. The charging time of the charger with the BRC technique has been

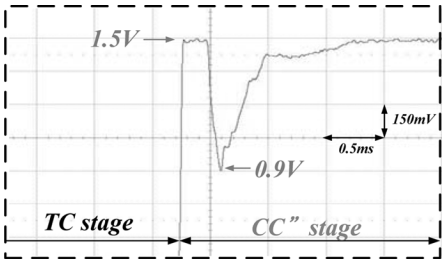

Fig. 18. Waveform of the $V_{\rm SET}$ voltage during the detection period.

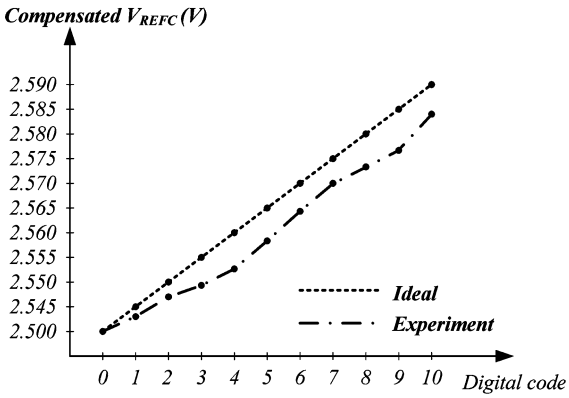

Fig. 19. Comparison of the shift reference voltage between the simulation and experimental results.

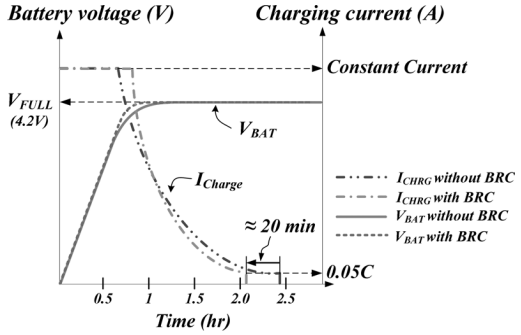

Fig. 20. Comparison of the $I_{\rm CHRG}$ charging current and the $V_{\rm BAT}$ battery voltage of the charger with and without the BRC technique.

shortened by about 20 min. In other words, the fast-charging performance is achieved by the BRC technique.

V. Conclusion

This paper has proposed a smooth transition method from the CC to the CV stage for the Li-ion charger. Due to the external parasitic resistance of the Li-ion battery-pack system, the conventional charger circuit switches from the CC to the CV stage without fully charging the cell to the rated-voltage value. The degrading current at the CV stage wastes a lot of time to fully charge the battery. Therefore, the concept of the BRC technique can achieve a nearly full charge at the CC stage but not at the CV stage owing to the larger charging current. That is, the proposed circuit is to redistribute the operation periods of the CC and CV stages in the charge process. The life cycle of the battery is not affected by the BRC method. The new BRC technique applied to the charger can speed up the charging time of the Li-ion battery. It can dynamically estimate the external resistance of the battery-pack system to extend the period of the CC stage to achieve a fast-charging response. The experimental results show that the period of the CC stage can be extended to about 40% of that of the original design. That is, the charger with the BRC technique can smoothly transit from the CC to the CV stage and have the fast-charging performance.

Acknowledgment

The authors would like to thank the Industrial Technology Research Institute and Chunghwa Picture Tubes, Ltd. for their help.

References

[1] M. Chen and G. A. Rincón-Mora, "Accurate, compact, and power-efficient Li-ion battery charger circuit," *IEEE Trans. Circuits Syst. II, Exp. Briefs*, vol. 53, no. 11, pp. 1180–1184, Nov. 2006.

[2] M. J. Isaacson, R. P. Hollandsorth, P. J. Giampaoli, F. A. Linkowaky, A. Salim, and V. L. Teofilo, "Advanced lithium ion battery charger," in *Proc. 15th Annu. Battery Conf. Appl. Adv.*, Jan. 2000, pp. 193–198.

[3] C.-C. Tsai, C.-Y. Lin, Y.-S. Hwang, W.-T. Lee, and T.-Y. Lee, "A multi-mode LDO-based Li-ion battery charger in 0.35 μm CMOS technology," in *Proc. IEEE Asia-Pacific Conf. Circuits Syst.*, Dec. 2004, pp. 49–52.

[4] Y.-S. Hwang, S.-C. Wang, F.-C. Yang, and J.-J. Chen, "New compact CMOS Li-ion battery charger using charge-pump techniques for portable applications," *IEEE Trans. Circuits Syst. I, Reg. Papers*, vol. 54, no. 4, pp. 705–712, Apr. 2007.

[5] J. Buxton, "Li-ion battery charging requires accurate voltage sensing," *Anal. Devices Anal. Dialog.*, vol. 31, no. 2, pp. 3–4, 1997.

[6] H. Vaidyanathan and G. Rao, "Electrical and thermal characteristics of lithium-ion cells," in *Proc. 14th Annu. Battery Conf. Appl. Adv.*, 1999, pp. 79–84.

[7] J. Lopez, M. Gonzalez, J. C. Viera, and C. Blanco, "Fast-charge in lithium-ion batteries for portable applications," in *Proc. 26th Annu. INTELEC*, Sep. 2004, pp. 19–24.

[8] A. M. Rahimi, "A lithium-ion battery charger for charging up to eight cells," in *Proc. IEEE Conf., Vehicle Power Propulsion*, 2005, pp. 131–136.

[9] S. Dearborn, "Charging Li-ion batteries for maximum run times," *Power Electron. Technol. Mag.*, vol. 31, no. 4, pp. 40–49, Apr. 2005.

[10] F. Lima, J. N. Ramalho, D. Tavares, J. Duarte, C. Albuquerque, T. Marques, A. Geraldes, A. P. Casimiro, G. Renkema, J. Been, and W. Groeneveld, "A novel universal battery charger for NiCd, NiMH, Li-ion and Li-polymer," in *Proc. Eur. Solid-State Circuits Conf.*, 2003, pp. 209–212.

[11] *"LTC1733: Monolithic Linear Lithium-Ion Battery Charger With Thermal Regulation,"* Linear Technol., Milpitas, CA, 2001 [Online]. Available: http://www.linear.com/

[12] R. Saint-Pierre, "A dynamic voltage-compensation technique for reducing charge time in lithium-ion batteries," in *Proc. 15th Annu. Battery Conf. Appl. Adv.*, Jan. 2000, pp. 179–184.

[13] J. Ramirez-Angulo, R. G. Carvajal, A. Torralba, J. Galan, A. P. Vega-Leal, and J. Tombs, "The flipped voltage follower: A useful cell for low-voltage low-power circuit design," *IEEE Trans. Circuits Syst. I, Reg. Papers*, vol. 52, no. 7, pp. 1276–1291, Jul. 2005.

[14] I. Padilla, J. Ramirez-Angulo, R. G. Carvajal, and A. Lopez-Martin, "Highly linear V/I converter with programmable current mirrors," in *Proc. IEEE ISCAS*, May 2007, pp. 941–944.

[15] H.-W. Huang, K.-H. Chen, and S.-Y. Kuo, "Dithering skip modulation, width and dead time controllers in highly efficient DC–DC converters for system-on-chip applications," *IEEE J. Solid-State Circuits*, vol. 42, no. 11, pp. 2451–2465, Nov. 2007.

Chia-Hsiang Lin was born in Taipei, Taiwan, in 1984. He received the B.S. and M.S. degrees in electrical and control engineering from National Chiao Tung University, Hsinchu, Taiwan, in 2006 and 2008, respectively.

He is currently working in Richtek, Ltd., Hsinchu. His research area includes the projects of chargers, and dc–dc converters at the Low Power Mixed Signal Laboratory. His research interests are low-dropout regulators, dc–dc converters, and analog integrated-circuit designs.

Chun-Yu Hsieh was born in Taichung, Taiwan. He received the B.S. degree in electrical and control engineering from National Chiao Tung University, Hsinchu, Taiwan, in 2004, where he is currently working toward the Ph.D. degree in electric and control engineering in the Department of Electrical Engineering and Institute of Electrical Control Engineering.

His research area includes many projects of LED driver ICs and power management ICs at the Low Power Mixed Signal Laboratory. His interests include power management circuit designs, LED driver ICs, and analog integrated-circuit designs.

Ke-Horng Chen (M'04–SM'09) received the B.S., M.S., and Ph.D. degrees in electrical engineering from National Taiwan University, Taipei, Taiwan, in 1994, 1996, and 2003, respectively.

From 1996 to 1998, he was a part-time IC Designer with Philips, Taipei. From 1998 to 2000, he was an Application Engineer with Avanti, Ltd., Taiwan. From 2000 to 2003, he was a Project Manager with ACARD, Ltd., where he was engaged in designing power management ICs. He is currently an Associate Professor with the Department of Electrical Engineering and Institute of Electrical Control Engineering, National Chiao Tung University, Hsinchu, Taiwan, where he organized the Mixed-Signal and Power Management IC Laboratory. He is an author or a coauthor of more than 80 papers published in journals and conferences and is a holder of several patents. His current research interests include power management ICs; mixed-signal circuit designs; display algorithm and driver designs of liquid crystal display TV; red-, green-, and blue-color sequential backlight designs for optically compensated bend panels; and low-voltage circuit designs.